Journal of Colloid and Interface Science **230,** 254–267 (2000)
doi:10.1006/jcis.2000.7075, available online at http://www.idealibrary.com on IDEAL®

Kinetics of Cream Formation by the Mechanism of Consolidation in Flocculating Emulsions

Tatiana D. Dimitrova,* Theodor D. Gurkov,*,[1] Nikolina Vassileva,* Bruce Campbell,† and Rajendra P. Borwankar†

*Laboratory of Chemical Physics Engineering,[2] University of Sofia, Faculty of Chemistry, James Bourchier Avenue 1, Sofia 1164, Bulgaria; and †Kraft Foods, Inc., Technology Center, 801 Waukegan Road, Glenview, Illinois 60025

Received September 17, 1999; accepted July 5, 2000

In this work we propose a theoretical description of the process of creaming of batch emulsions when a sharp boundary exists between a clear serum phase and the sedimenting drops. The creaming is represented as a continuous consolidation of partially aggregated network. The treatment reproduces correctly the trend for gradually decreasing rate of sedimentation as time goes on. The theoretical results are compared quantitatively with experimental measurements of the creaming rate. Oil-in-water systems, stabilized by proteins (β-lactoglobulin (BLG), bovine serum albumin, and mixtures BLG + β-casein) were investigated. Faster creaming is attributed to larger size of the sedimenting objects (flocs of emulsion droplets). In systems obeying the creaming mechanism with sharp boundary (SB) the flocs are smaller when the protein concentration is higher. This supports the hypothesis for the stabilizing role of the excess amount of protein (forming lumps and multilayers on the interface). Theoretical analysis demonstrates that the formation of flocs by gravitational coagulation is a much faster process than the consolidation of the cream. Hence, the dispersions first flocculate and then cream. With increasing β-casein content in mixtures BLG + β-casein the emulsions depart from the SB-type behavior and are characterized by the presence of small nonflocculated droplets, which do not sediment (the serum is turbid and the boundary with the concentrated dispersion is diffuse, DB behavior). This is connected with hindered flocculation, perhaps due to β-casein's augmented ability to prevent droplet aggregation.

Key Words: **emulsions; creaming; flocculation; stabilization by proteins; sedimentation kinetics; aggregated networks.**

1. INTRODUCTION

Emulsions containing micrometer-size drops are thermodynamically unstable systems. Nevertheless, their shelf life may be as long as months and years, provided that kinetic stability is achieved by proper choice of surfactant(s). There are three processes chiefly responsible for emulsion degradation: (i) coalescence of the droplets, which leads to separation of the two bulk liquid phases, (ii) creaming due to drop sedimentation, and (iii) Ostwald ripening. In this work we shall be concerned only with emulsions that are stable with respect to coalescence, but are subject to creaming (in the absence of Ostwald ripening).

Since the problem of emulsion stability is very important from a practical point of view, it has attracted much attention in the literature. Experimentally, kinetics of creaming has been studied by ultrasound velocity scanning technique (1–4), which gives the profile of the volume fraction along the height of the emulsion column. The change in the profile as a function of time is usually monitored. Computer simulations of the creaming process have also been offered (5). Some theoretical considerations for the conditions during creaming (drop velocity, volume fraction distribution) were discussed in Ref. (6). Dukhin and Sjoblom (7) reviewed recent advances in the theory of Brownian and gravity-induced flocculation and the relation of the latter to creaming.

In general, it has been recognized that the rate of creaming is closely related to the extent of droplet flocculation (1–4). This is easily understandable, because flocs of droplets move as distinct objects in the suspension and experience larger total buoyancy force in comparison with the individual droplets. Hence, flocculated emulsions should cream faster.

Manoj *et al.* (3) observed two different types of creaming in oil-in-water (o/w) emulsions containing polysaccharides. The first one is characterized by absence of a clear serum phase—the lower portion of the dispersion remains opaque while a concentrated cream layer develops at the top of the sample. The boundary between the serum and the creaming droplets is very hazy and difficult to monitor visually. This behavior is typical for highly polydisperse emulsions in which part of the droplets would not flocculate: individual drops and small aggregates move independently to the top of the container (3), and the smallest entities do not sediment at all. In contrast, in the second type of creaming there exists a sharp and clear boundary between the concentrated sedimenting emulsion and the serum layer at the base of the sample. The serum can be clear or only slightly turbid. In Ref. (3) this kind of behavior was attributed to systems with high degree of flocculation, sufficient to produce a space-spanning structure.

These findings are confirmed by our own observations with o/w emulsions stabilized by proteins (see below). The present paper is focused on the creaming mechanism with sharp boundary (SB). Our aim is to investigate the latter mechanism in a more

[1] To whom correspondence should be addressed. E-mail: tg@LTPH.BOL.BG.

[2] Formerly: Laboratory of Thermodynamics and Physico-Chemical Hydrodynamics.

0021-9797/00 $35.00

deep and quantitative manner. For this purpose we develop a theoretical description of the settling process in an emulsion which contains monodisperse objects (drops, or clusters thereof). Our treatment takes into account the fact that the dispersion is flocculated. We basically follow the approach proposed by Buscall (8), Buscall and White (9), and Landman and White (10), who consider consolidation of weakly aggregated particulate networks. Equations governing the kinetics of creaming, in particular, the time evolution of the spatial distribution of the particle concentration in a flocculated sedimenting dispersion, were derived in Refs. 8 and 9. However, no concrete solutions with appropriate boundary conditions have been provided for the creaming rate. Our main task here will be to formulate a complete mathematical problem and to carry out numerical calculations from which one can gain relevant information about the process of cream formation. The local volume fraction, ϕ, is found as a function of position and time, by solving the respective partial differential equation. We specify the boundary conditions, and determine how the boundary between the clear supernatant (serum) and the emulsion is moving with time. Quantitative comparison of the theoretical results with experimental measurements of the creaming rate is offered. Experimental curves for the time evolution of the separated cream volume are fitted. Good agreement is obtained for several o/w emulsion systems stabilized by proteins. In such a way the peculiar behaviour of the creaming curves is explained (the rate of sedimentation gradually decreases as time goes on). Faster creaming in systems with lower protein content is attributed to a greater extent of flocculation.

2. THEORY

In a sedimenting suspension the particles experience (i) gravitational force (buoyancy) and (ii) viscous resistance (drag), which opposes the motion because of the friction with the liquid (8–11). When only individual Brownian particles are present in a nonflocculated dispersion, one has to take into account also (iii) the so-called "thermodynamic force" (11). The latter arises from the nonuniform distribution of particles and is actually due to diffusion and Brownian motion. This force is directed from higher to lower osmotic pressure (cf. Eq. (12.5.5) in Ref. (11)).

As pointed out by Buscall and White (9), in the case of flocculation and above a certain critical concentration, ϕ_g, the clusters of particles become overcrowded (i.e., start touching each other), and form a kind of a space-filling network. Gravity causes this "gel" to consolidate irreversibly. Typically, the critical volume fraction ϕ_g is as small as 0.05 if the coagulation has been proceeding by a rapid perikinetic mechanism (i.e., by diffusion-controlled aggregation into a deep primary minimum of the potential energy) (8).

In flocculated dispersions the "thermodynamic force" is obviously irrelevant, because it would imply free motion of small individual particles. (The flocs are usually big enough that they do not experience significant Brownian force.) Instead, one introduces the concept of "particle pressure," p (8, 9). The basic idea here is that when particles (flocs) move during the process of cream compaction some contacts between the drops have to be disrupted, and in addition, the particles that slide toward each other are subjected to collisions with their neighbors. The sliding itself is accompanied by resistance to shearing motion in the interfacial layers and in the intervening thin liquid films. All these short-range interactions give rise to an effective particle pressure. It has the meaning of osmotic pressure, which includes the collisions and the short-range interactions between the particles. In our considerations the term "particle" is used to designate an aggregate of liquid drops (in the case of partially flocculated emulsion).

It is common to assume that p is a function of the local volume fraction only, $p = p(\phi)$ (8, 9). This is equivalent to regarding p as being independent from the deformation rate during compaction of the cream (sediment). One can now utilize the experimentally established explicit relation $p(\phi) \sim \phi^4$ (see Ref. 8 and the literature cited therein). This functional dependence has been confirmed to hold for $\sim 0.05 < \phi < \sim 0.3$ (see Fig. 7 in Ref. 8).

Let us consider the system depicted in Fig. 1. The direction of the coordinate axis z is chosen to be opposite to the velocity of particle motion. In general, the sedimenting suspension divides into several zones. The supernatant, or serum, represents a more or less clear fluid, $\phi = 0$. A region of maximum concentration exists at the top of the cream (in the case of o/w emulsion whose oil phase has lower density than water). We denote the maximum possible volume fraction by $\phi_{\max}$. Within the consolidating dispersion ϕ is a function of both position and time, $\phi(z, t)$. The boundary between the serum and the suspension is

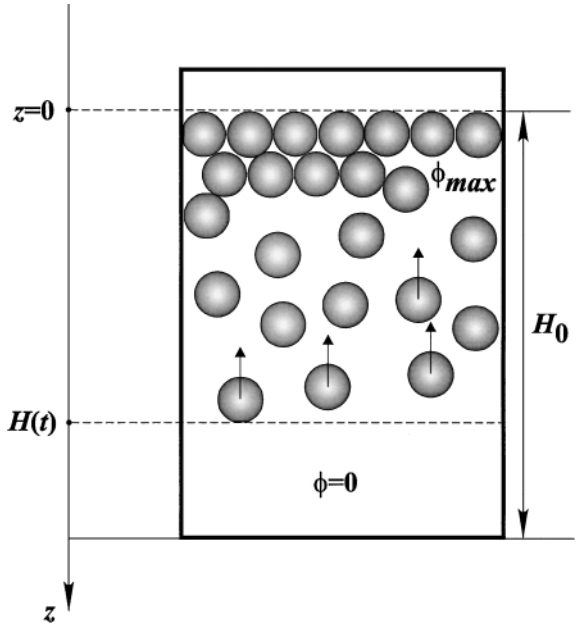

FIG. 1. Sketch of a creaming emulsion.

usually sharp, which allows one to monitor its motion in a real batch system simply by visual observation. The position of this boundary, i.e., the height of the column that contains the particles, will be denoted by $H(t)$ (Fig. 1). Our goal here will be to compute the function $H(t)$ theoretically, and compare with the experiment. As will be shown below, the volume fraction in the cream gradually decreases with increasing distance from the top, so that there is no distinct layer where $\phi = \phi_{\max}$ (no sharp boundary can be discerned between the most dense sediment and the more diluted regions in the emulsion).

The material balance of the dispersed phase in the region $z < H(t)$ (Fig. 1) states that

$$\frac{\partial \phi}{\partial t} - \frac{\partial}{\partial z}(\phi u) = 0, \qquad [1]$$

where u is the magnitude of the particle velocity (8–11). Equation [1] is valid for a monodisperse sample; i.e., we do not consider aggregation going on simultaneously with the sedimentation. Instead, it is assumed that the flocs have already been formed, and now they just settle upward. In quasistationary conditions the viscous drag counterbalances the driving force, $\mathbf{F}_{\mathrm{d}}$, exerted on the particle. $\mathbf{F}_{\mathrm{d}}$ is a superposition of buoyancy and particle pressure gradient (8):

$$F_{\mathrm{d}} = |\mathbf{F}_{\mathrm{d}}| = -\Delta\rho g v - \frac{1}{n}\frac{\partial p}{\partial z}. \qquad [2]$$

Here $\Delta\rho$ is the density difference, g is the gravity acceleration, v is the volume of one particle, and n is the number concentration of particles, $n = \phi/v$. The velocity u can now be determined from the balance between $\mathbf{F}_{\mathrm{d}}$ and the viscous resistance $u\zeta/K(\phi)$,

$$u = \frac{K(\phi)}{\zeta}\left[\Delta\rho g v + \frac{1}{n}\frac{\partial p}{\partial z}\right], \qquad [3]$$

where $K(\phi)/\zeta$ represents the mobility. ζ is the friction coefficient of an isolated particle in an infinite medium. For spheres $\zeta = 6\pi\eta a$ (η is the dynamic viscosity of the fluid, and a is the particle radius). The function $K(\phi)$ formally accounts for the increase of the viscous drag due to crowding of the particles; in other words, $K(\phi)$ characterises the hydrodynamic interactions in the suspension. Inserting Eq. [3] into [1] gives

$$\frac{\partial \phi}{\partial t} - \frac{v}{\zeta}\frac{\partial}{\partial z}\left\{K(\phi)\frac{\mathrm{d}p}{\mathrm{d}\phi}\frac{\partial \phi}{\partial z}\right\} - \frac{\Delta\rho g v}{\zeta}\frac{\partial}{\partial z}\{\phi K(\phi)\} = 0. \qquad [4]$$

This is the governing equation for the process of sedimentation. When writing the second term, we have used the fact that p depends on z only implicitly, through ϕ: $p = p[\phi(z, t)]$. Equation [4] can be cast in dimensionless form by scaling the z-coordinate with the column height $H(t)$. We introduce new variables,

$$\tilde{z} \equiv \frac{z}{H(t)}, \qquad \tilde{t} \equiv \frac{t}{H_0/U_0}, \qquad \tilde{p} \equiv \frac{p}{\Delta\rho g H_0}, \qquad [5]$$

where

$$U_0 = \frac{\Delta\rho g v}{\zeta} \qquad [6]$$

is the settling velocity of an isolated particle. H_0 denotes the initial height of the emulsion column: $H_0 = H(t = 0)$. In view of Eqs. [5], we now have $\phi = \phi[\tilde{z}(z, t), \tilde{t}(t)]$ and

$$\left(\frac{\partial \phi}{\partial z}\right)_t = \frac{1}{H(t)}\left(\frac{\partial \phi}{\partial \tilde{z}}\right)_{\tilde{t}},$$

$$\left(\frac{\partial \phi}{\partial t}\right)_z = \frac{U_0}{H_0}\left(\frac{\partial \phi}{\partial \tilde{t}}\right)_{\tilde{z}} - \tilde{z}\left(\frac{\partial \phi}{\partial \tilde{z}}\right)_{\tilde{t}}\frac{1}{H(t)}\frac{\mathrm{d}H}{\mathrm{d}t},$$

so that Eq. [4] transforms to read

$$\frac{H(t)}{H_0}\frac{\partial \phi}{\partial \tilde{t}} - \frac{H_0}{H(t)}\frac{\partial}{\partial \tilde{z}}\left\{K(\phi)\frac{\mathrm{d}\tilde{p}}{\mathrm{d}\phi}\frac{\partial \phi}{\partial \tilde{z}}\right\} - \frac{\partial}{\partial \tilde{z}}\{\phi K(\phi)\} - \tilde{z}\frac{\partial \phi}{\partial \tilde{z}}\frac{\mathrm{d}}{\mathrm{d}\tilde{t}}\left(\frac{H}{H_0}\right) = 0. \qquad [7]$$

This complicated equation contains two unknown functions, $\phi(\tilde{z}, \tilde{t})$ and $H(\tilde{t})$. Therefore, we need one more equation to connect ϕ and H. The conservation of mass of the dispersed phase requires that $\int_0^{H(t)} \phi(z, t)\,\mathrm{d}z$ should remain constant during the process of sedimentation. If at the initial moment $t = 0$ the suspension was homogeneous, with $\phi = \phi_0$ for $0 < z < H_0$, then

$$\frac{H(\tilde{t})}{H_0} = \frac{1}{\int_0^1 \frac{\phi(\tilde{z}, \tilde{t})}{\phi_0}\,\mathrm{d}\tilde{z}} \qquad [8]$$

at any arbitrary $\tilde{t}$. Equation [8] allows us to determine $H(\tilde{t})$ from the profile of the volume fraction, $\phi(\tilde{z}, \tilde{t})$.

Let us now discuss the boundary and initial conditions to the partial differential equation [7]. At each moment of time we impose the following boundary conditions:

$$\phi(\tilde{z} = 0, \tilde{t}) = \phi_{\max}, \qquad \phi(\tilde{z} = 1, \tilde{t}) = 0. \qquad [9]$$

The initial condition for $H(\tilde{t})$ is simply $H(0) = H_0$, whereas the derivative $(\mathrm{d}H/\mathrm{d}\tilde{t})_{\tilde{t}=0}$ (which is also needed, cf. Eq. [7]) can be found if one realizes that at $\tilde{t} = 0$ the spatial gradient of ϕ has not yet been developed in the emulsion volume, and the term $\partial p/\partial z$ then drops off from Eq. [3]. Since at $\tilde{t} = 0$ the boundary starts moving with velocity $(\mathrm{d}H/\mathrm{d}t)|_{t=0} = -u|_{t=0}$, Eqs. [3] and [6] yield

$$\left.\frac{\mathrm{d}H}{\mathrm{d}t}\right|_{t=0} = -U_0 K(\phi_0), \quad \left[\frac{\mathrm{d}}{\mathrm{d}\tilde{t}}\left(\frac{H}{H_0}\right)\right]_{\tilde{t}=0} = -K(\phi_0). \qquad [10]$$

We adopt the following initial distribution of the volume fraction ϕ (see below for discussion):

$$\phi(\tilde{z} = 0, \tilde{t} = 0) = \phi_{\max}, \qquad \phi(0 < \tilde{z} < 1, \tilde{t} = 0) = \phi_0, \qquad \phi(\tilde{z} = 1, \tilde{t} = 0) = 0. \qquad [11]$$

This may seem somewhat artificial. However, it is still realistic because the characteristic velocity of particle motion, $U_0 = (2\Delta\rho g a^2)/(9\eta)$, is relatively high, e.g., about 6.5×10^{-4} cm/s for a sphere with radius $a = 5$ μm, with $\Delta\rho = 0.12$ g/cm^3 (water/xylene), $g = 981.55$ cm/s^2, $\eta = 0.01$ g/(cm · s). Thus, the time for one particle to pass a distance equal to its diameter is rather short—of the order of 1 s. Hence, just after a homogeneous dispersion is loaded in a vessel the lowest layer (Fig. 1) will be depleted from particles, and the uppermost layer will reach close packing at $\phi_{\max}$. As far as we are interested in the long-term behavior of emulsions (at a time scale much larger than a second), Eqs. [11] represent an appropriate initial condition for ϕ.

The dimensionless particle pressure is written as

$$\tilde{p}(\phi) = \tilde{p}_0(\phi/\phi_0)^4, \qquad [12]$$

where $\tilde{p}_0$ stays as a model parameter in our theory. For the function $K(\phi)$ we adopt the experimentally established relation valid for hard spheres (see Ref. 8 for details):

$$K(\phi) = (1-\phi)^{5.4}. \qquad [13]$$

Let us mention here that slight modifications in the power laws ([12], [13]) within the experimentally established permissible ranges (8–10) do not alter our results. We tested $\tilde{p}(\phi) \sim \phi^{3.6}$ and $K(\phi) = (1-\phi)^5$ and obtained essentially the same theoretical creaming curves.

3. NUMERICAL CALCULATIONS

We solve Eq. [7] numerically, using a semiimplicit finite difference scheme. The coordinate and time are discretized by small intervals ($\Delta\tilde{z} = 0.01$ and $\Delta\tilde{t} = 10^{-4}$–$10^{-6}$). The derivatives of ϕ are expressed as

$$\frac{\partial\phi(\tilde{z},\,\tilde{t}+\Delta\tilde{t})}{\partial\tilde{t}} = \frac{\phi(\tilde{z},\,\tilde{t}+\Delta\tilde{t}) - \phi(\tilde{z},\,\tilde{t})}{\Delta\tilde{t}}$$

$$\frac{\partial\phi(\tilde{z},\,\tilde{t}+\Delta\tilde{t})}{\partial\tilde{z}} = \frac{\phi(\tilde{z}+\Delta\tilde{z},\,\tilde{t}+\Delta\tilde{t}) - \phi(\tilde{z}-\Delta\tilde{z},\,\tilde{t}+\Delta\tilde{t})}{2\Delta\tilde{z}} \qquad [14]$$

$$\frac{\partial^2\phi(\tilde{z},\,\tilde{t}+\Delta\tilde{t})}{\partial\tilde{z}^2} = \frac{\phi(\tilde{z}+\Delta\tilde{z},\,\tilde{t}+\Delta\tilde{t}) - 2\phi(\tilde{z},\,\tilde{t}+\Delta\tilde{t}) + \phi(\tilde{z}-\Delta\tilde{z},\,\tilde{t}+\Delta\tilde{t})}{(\Delta\tilde{z})^2}.$$

All coefficients which multiply these derivatives in Eq. [7] are taken at the instant $\tilde{t}$. Equation [7] is nonlinear; the term $(\partial\phi/\partial\tilde{z})^2$ is represented as a product of one derivative referring to the moment $\tilde{t}+\Delta\tilde{t}$ and the other one taken at $\tilde{t}$. In this manner we obtain a linear set of algebraic equations for the unknown quantities $\phi(\tilde{z}_k, \tilde{t}+\Delta\tilde{t})$ $(k = 1, 2, \ldots)$, since $\phi(\tilde{z}_k, \tilde{t})$ have been determined at the preceding time step. The linear system has a tridiagonal matrix of coefficients, and is solved by Gauss elimination method (Ref. (12)).

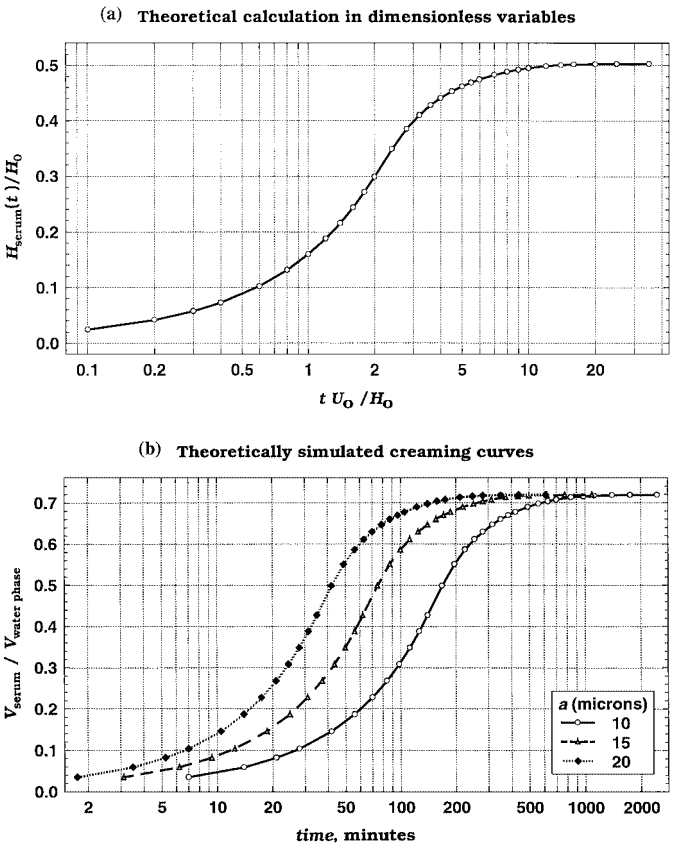

FIG. 2. (a) Calculated height of clear serum separated from a batch dispersion. $\phi_0 = 0.30$, $\phi_{\max} = 0.64$ (value which corresponds to random packing of hard spheres (11)), $\tilde{p}_0 = 0.002$. (b) Calculated creaming curves, representing the time dependence of the serum volume scaled with the total volume of the aqueous phase in the emulsion. The three sets of data have been generated from one and the same curve in dimensionless variables (that from a), taking three different particle sizes: 10, 15, and 20 μm. $\phi_0 = 0.30$, $\phi_{\max} = 0.64$.

Figure 2 shows some data obtained by computation according to Eq. [7]. In Fig. 2a the creaming rate is characterized by the height of the separated column of serum, plotted vs dimensionless time ($H_{\text{serum}}(t) = H_0 - H(t)$ in the notation of Fig. 2a). We observe a typical behavior of gradually decreasing rate of sedimentation. Finally the dispersion reaches equilibrium and stops consolidating altogether. Then, the gradient in the particle pressure, $\partial p/\partial z$, which is brought about by the gradient of ϕ, as $p = p(\phi(z,t))$, counterbalances gravity throughout the whole cream (cf. Eq. [3]). For the sake of illustration, we have chosen the value of $\tilde{p}_0$ in Fig. 2 arbitrarily. In Section 5 some experimental data for the creaming rate will be fitted by adjusting the model parameters in the theory.

Figure 2b is drawn in physical variables, in the scale usually used to present measured creaming curves. The three sets of data in Fig. 2b were calculated from one and the same curve in dimensionless variables, namely, that from Fig. 2a. We only switched

to the respective quantities on the axes, choosing three different particle sizes ($a = 10$, 15, and 20 μm). With emulsions "particle" is supposed to mean either an individual drop or a stiff aggregate of not too many drops, i.e., an object which can move and interact with its neighbors. In dimensionless variables (Fig. 2a) the results do not depend on the particle radius, a, because the latter is included in the scaling on the abscissa.

One notices that, with all other parameters being the same, different particle sizes give curves with similar shapes which are shifted with respect to each other on the log(time) axis (Fig. 2b). A given amount of serum is released earlier when a is larger (this of course may be anticipated). Another aspect of the creaming process (observed in real emulsion systems) is the existence of "delay time"—a period before the intensive sedimentation starts. In general, this delay time may be due to two reasons: (i) slower compactification of the cream in the beginning, which is predicted by our theory from Section 2 (cf. Fig. 2b) ("hydrodynamic" delay time); (ii) the time needed for the dispersion to aggregate. We investigated the latter possibility by estimating the rate of orthokinetic flocculation theoretically. The results are presented in Section 6. It is proved that for a typical emulsion with micrometer-size droplets (in the absence of potential barriers) the time required for formation of aggregates comprising dozens of particles is very short.

In Fig. 3 we plot calculated profiles of the volume fraction in a sedimenting dispersion. At relatively not very long times ($\tilde{t} = 1.6$, for instance, which corresponds to real time $\sim$112 min with $H_0 = 11$ cm, $\Delta\rho = 0.12$ g/cm^3 (water/xylene), $\eta = 0.01$ g/(cm $\cdot$ s) (water), $g = 981.55$ cm/s^2, $a = 10$ μm), there is a region where $\phi = \phi_0$. In addition, ϕ turns out to decrease monotonously from $\phi_{\max}$ to ϕ_0, and no distinct layer with $\phi = \phi_{\max}$ exists. Later on, the region where $\phi = \phi_0$ disappears. A similar trend was noticed by Dickinson *et al.* (1), who used an ultrasound velocity scanning technique to measure the distribution of dispersed phase in emulsions stabilized by sodium caseinate. The authors of Ref. 1 found that in a 35 vol% tetradecane/water emulsion at earlier times there is a region with $\phi = \phi_0$, whereas at very long times the cream is more or less homogeneous, with $\phi > \phi_0$ throughout.

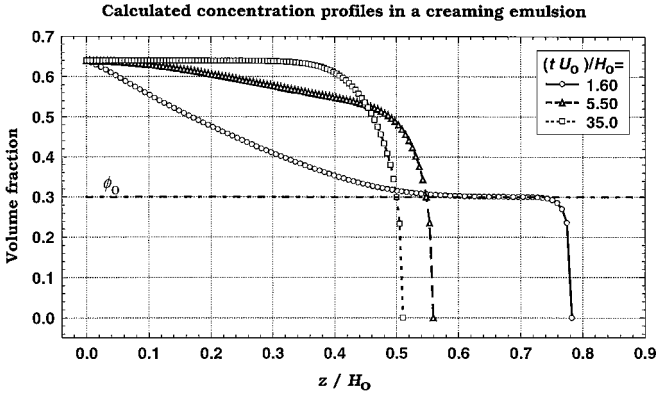

FIG. 3. Spatial distribution of the particle concentration in a consolidating dispersion at three different time moments. $\phi_0 = 0.30$, $\phi_{\max} = 0.64$, $\tilde{p}_0 = 0.002$ (Eq. [12]).

In our case the final equilibrium state of the sediment (which roughly corresponds to $\tilde{t} = 35.0$ in Fig. 3) is a dense layer with $\phi = \phi_{\max}$, whose boundary at the side of the liquid is somewhat diffuse (due to the effect of the gradient $\partial p/\partial z$—see above).

4. EXPERIMENTAL

4.1. Materials

As oil phases in the emulsions we used xylene and soybean oil (commercial products). They were additionally purified by passing through a column filled with the chromatographic adsorbent Florisil-F101. The procedure was similar to that proposed by Gaonkar (13). Approximately 10 g of adsorbent were needed for each 50 ml of oil. The oil was kept in closed dark bottles in a dark dry place.

Aqueous phase was prepared using water purified by a Millipore Milli-Q unit (resistance 18.2 MΩ cm^{-1}). The emulsion stabilizers were proteins: β-lactoglobulin (BLG), β-casein, and two types of bovine serum albumin (not purified from fatty acids, BSA-non-FAF, and essentially fatty acid free, BSA-FAF). They were purchased from Sigma Co., and were used as received. The concentration of electrolyte was adjusted with NaCl (Merck), preliminarily baked for 5 h at 450°C in order to remove all organic contaminants. The acidity was regulated by adding the appropriate amount of HCl (Sigma, analytical grade). When pH 7 was needed, it was maintained by phosphate buffer with a total concentration of 3–6 mM.

4.2. Methods

Preparation of the emulsion samples. We used a rotor-stator homogenizer Ultra Turrax T25 (Janke & Kunkel GmbH, IKA-Labortechnik). The dispersing tool was introduced in a 200-ml laboratory beaker containing a 70-ml aqueous phase. The disperse phase (30 ml oil) was poured in carefully, during an approximately 10-s period, with continuous mixing (at 8000 rpm). Once the disperse phase had been added, the emulsion was homogenized for another 3 min (at 25,000 rpm). In all experiments the total amount of both phases was 100 ml. The samples were stored in closed vessels.

Following the creaming of batch emulsions. Those investigations were performed with emulsion samples stored in equal, sealed graduated glass cylinders (of volume 25 ml, inner diameter 17 mm). The boundaries of the layers in the creamed samples were observed in transmitted light. Sometimes we noticed a small amount of foam floating above the emulsions in the beginning stages; that foam was not included in the measured volume.

"Secondary creaming" curves were obtained in the following manner: After the emulsions had reached a final state with a more or less constant amount of the separated cream, the content of the glass cylinders was shaken by gently turning the samples

over, up and down 20 times. After that, we started accounting the volume of the newly separated cream.

Density measurements. Those were used to determine the volume fraction of oil in the cream (from which small samples were taken by pipet). The experiments were performed by means of AntonPAAR densitometer, model DM48, with accuracy of 0.0002 g cm^{-3}. Such a precision allows us to determine the volume fraction (in binary liquid mixtures or suspensions) with absolute error as small as 0.2%, if the density difference is of the order of 0.1 g cm^{-3}. We have to mention here that this is the minimum possible error, due to the accuracy of the apparatus. Actually, there may be also an additional (perhaps larger) error, associated with a variation in the composition when several specimens are taken independently from a certain place in the cream.

Determination of the droplet size distribution. We did not dilute the samples, in order to avoid the possibility of coalescence. The emulsions were observed in transmitted light, by means of a microscope (with objective $100\times/1.3$). The specimens were prepared by placing a small quantity of emulsion on a cytometric glass cell. The resolution of the light microscopy is 0.5–1 μm, which limits to some extent the precision of the size measurements.The obtained pictures were recorded with a high-resolution CCD camera (Sony) and digital memory VCR (Panasonic WV-5490). The recorded images were manually processed using a specially developed software, operating with TARGA+ graphic board (Truevision, USA). In all cases at least 400 droplets were counted for each size determination. In order to decrease the possibility for a systematic error, counting was performed in at least eight different randomly chosen frames. Every droplet was taken into account, even the smallest one (which was still visible). An example of size distribution histogram is presented in Fig. 6.

Dynamic light scattering measurements. We used Autosizer 4700C (Malvern Instruments, Ltd.), supplied with an argon laser (Innova, Coherent) operating at wavelength 488 nm, and a K7032 CE-8-multibit 128-channel correlator. This equipment was employed to determine particle sizes below ~ 1 μm, in emulsions and in protein solutions.

5. RESULTS AND COMPARISON BETWEEN THEORY AND EXPERIMENT

In our experiments we observed *two distinct types of emulsion creaming*. Hereafter we shall designate them as SB (sharp boundary) and DB (diffuse boundary) mechanisms, respectively.

5.1. Creaming According to the SB Mechanism

In this case the emulsion column divides into two clearly visible zones, $\phi \approx 0$ and $\phi > 0$, as shown schematically in Fig. 1. The lower phase (serum) is a more or less clear fluid, whereas the upper phase consists of emulsion and cream, and the volume fraction there is a continuous function of position and time, $\phi(z, t)$. The height $H(t)$ (Fig. 1) describes the position of the boundary between the cream and the clear serum. This is an experimentally measurable quantity, which was determined by us by visual observation.

We fitted our data for the rate of creaming, $H(t)$, using the particle pressure, p_0, and the average radius of the floating species, a, as two free parameters. The maximum volume fraction in the cream, $\phi_{\max}$, should also be known in order to run the calculation. However, $\phi_{\max}$ cannot be regarded as an adjustable parameter because from the experiment (cream volume and density measurements) we obtain the average volume fraction in the final state of the cream. It is plausible to choose $\phi_{\max}$ to be slightly higher than this average value of ϕ (since the cream is never entirely homogeneous in vertical direction). On the other hand, the simulations show that the solutions of Eqs. [7] and [8] practically do not depend on the exact value of $\phi_{\max}$.

The procedure for obtaining the fits in Fig. 4 is follows:

- First, from the experimental data for the final cream volume we find the average oil volume fraction in the cream, assuming that all droplets have sedimented. The latter assumption is realistic because the serum is more or less transparent, i.e., virtually free from droplets. This value of ϕ in the cream is found to coincide with what has been determined using density measurements (within the limits of the experimental accuracy). Then we suggest a value for $\phi_{\max}$, typically with about 0.2–0.4% higher than the experimental average cream volume fraction.
- Second, the parameter p_0 is determined (in dimensionless form it is $\tilde{p}_0 = p_0/[\Delta\rho g H_0]$). Once $\phi_{\max}$ is fixed, we run the theoretical computation and solve Eqs. [7] and [8] for very long times. The final state of the cream (which corresponds to the position of the plateau in the $H_{\text{serum}}(t)$ or $V_{\text{serum}}(t)$ plot, Fig. 2) has to coincide with the measurement, and this defines the value of $\tilde{p}_0$. Indeed, it turns out that the average final volume fraction in the cream depends on $\tilde{p}_0$: higher particle pressures lead to looser packing. Perhaps, this is due to restricted possibility for rearrangement of the particulate network.
- Finally, knowing $\phi_{\max}$ and $\tilde{p}_0$, we find the corresponding average size of the creaming objects for each emulsion, by adjusting the whole theoretical curve, $V_{\text{serum}}(t)$, to pass through all experimental points (Fig. 4). The effective diameter of the creaming particles, $2a_{\text{eff}}$, is very important from physical point of view, since it is directly connected with the degree of flocculation.

Figure 4 shows experimental data (points) for different systems whose creaming behavior corresponds to the SB mechanism. All curves in Fig. 4 represent theoretical fits. Evidently, the agreement between theory and experiment is quite good, which gives us a hint that the model described above is adequate for this particular case of creaming behavior. As a rule, the theoretically found values for the average sizes of the flocs (a_{eff}) are in accord with our microscopic observations. A typical floc in an emulsion stabilized by BLG is presented in Fig. 5a. Table 1

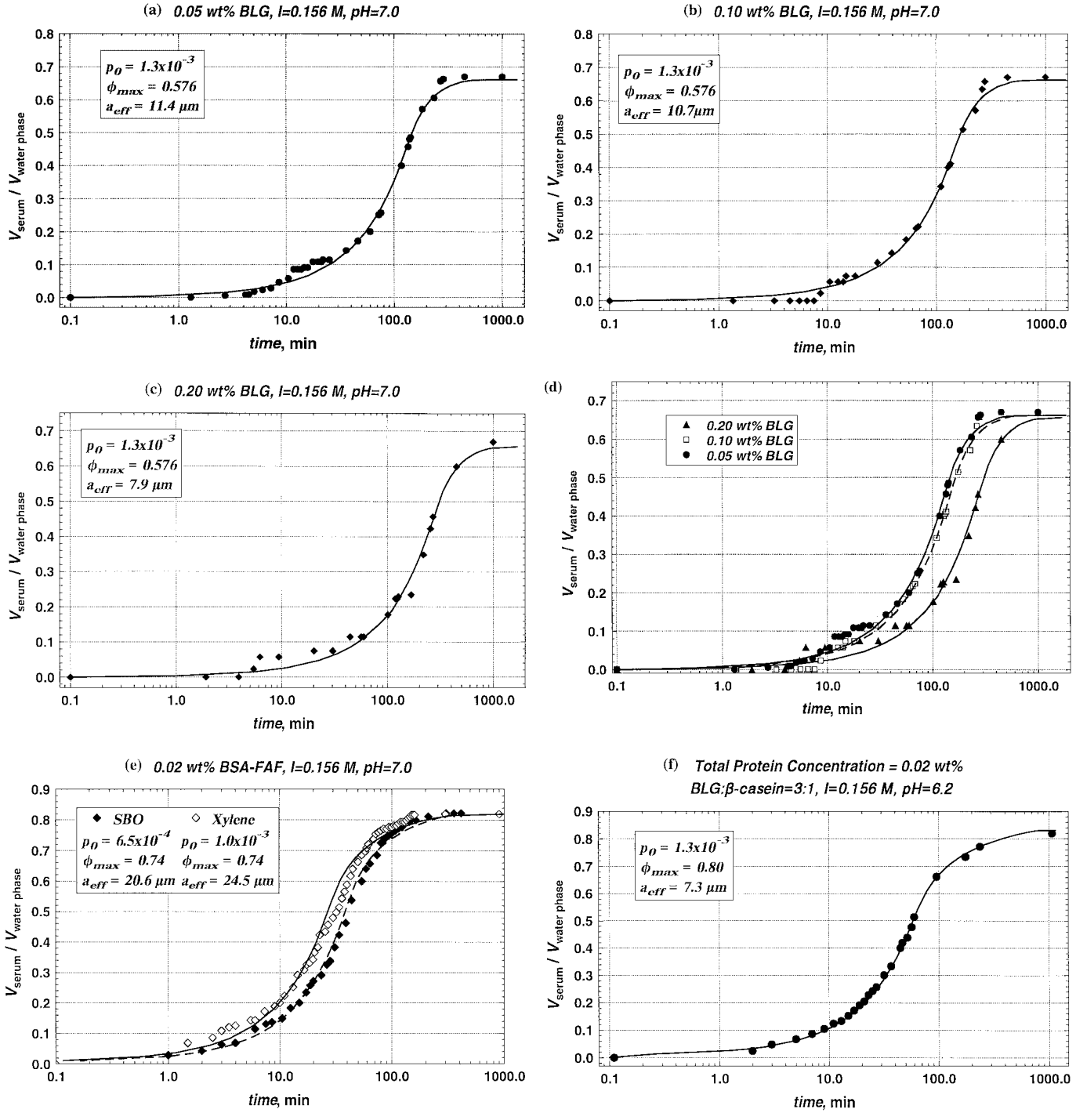

FIG. 4. Theoretically computed volume of the clear serum separated in batch emulsions, V_{serum}, scaled by the total volume of the aqueous phase, $V_{\text{water phase}}$ (the lines), and experimental measurements of the same quantity (the points). $V_{\text{serum}}/V_{\text{water phase}} = [1 - H(t)/H_0]/(1 - \phi_0)$. The emulsions are of o/w type, stabilized by proteins. The particular conditions are listed in each graph.

summarizes all fitting parameters determined in the studied systems. The number of the droplets in a floc (N in the last column of Table 1) has been calculated by assuming that the oil volume fraction in each floc is the same as that in the final cream of the corresponding emulsion. Information about the average size of the individual oil droplets (R_1) has been extracted from the images taken by microscopy.

Our theoretical considerations (in particular, Eq. [7]) are valid for monodisperse particles. This means that the flocculation process is supposed to be fast enough, so that it has already been

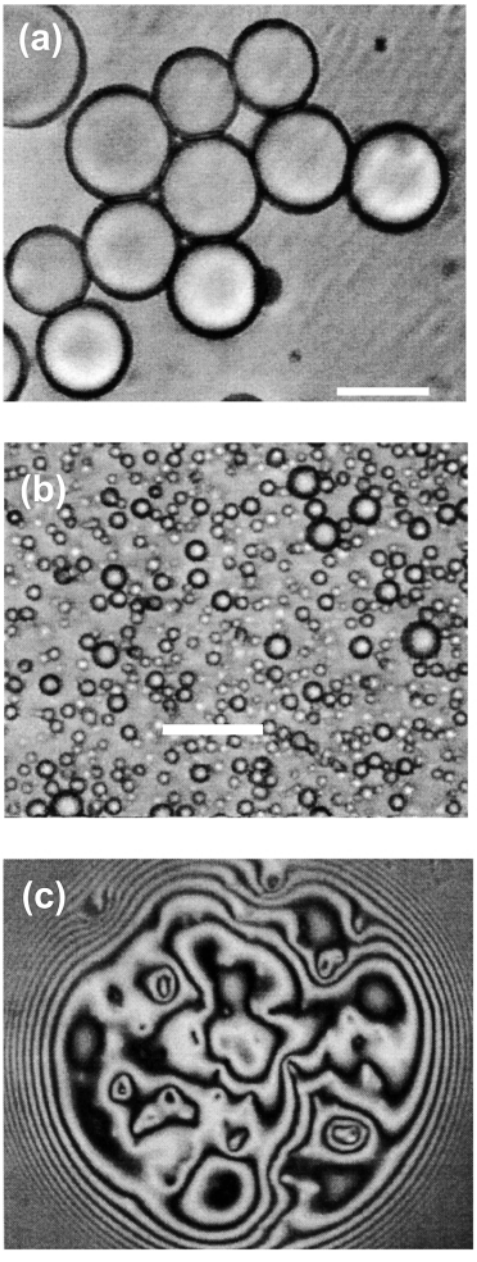

FIG. 5. (a) Floc in xylene/water emulsion, at 2 h after preparation. The system is stabilized with 0.02 wt% BLG, in the presence of 0.15 M NaCl. The bar on the picture corresponds to 10 μm. (b) Soybean oil/water emulsion containing 0.05 wt% β-casein in the aqueous phase (plus 0.15 M NaCl, pH 5.3). The reference bar corresponds to 20 μm. (c) Foam film with diameter $\sim$200 μm, stabilized by 0.02 wt% BLG, in the presence of 0.15 M NaCl (pH 5.4).

completed before the creaming takes place. In Section 6 below we provide a justification of this assumption, by numerical modeling of the rate of orthokinetic (buoyancy-driven) flocculation in an emulsion with mean drop radius of $\sim$3 μm.

Let us now discuss the most important conclusions for different particular cases of protein-containing systems.

5.1.1. BLG alone. One of the most intriguing features of the BLG-stabilized emulsions (Figs. 4a–4d and rows 1–3 in Table 1) is that with increasing protein concentration the floc size diminishes: compare the effective particle (floc) radius, a_{eff}, and the number of drops in a floc, N (Table 1). The data from Figs. 4a–4c are collected in Fig. 4d, where we compare the theoretical curves and the experimental points for all BLG concentrations. It is evident that the creaming curves have similar shapes, but those that correspond to higher content of BLG are shifted to the right of the log(time) axis (Fig. 4d). This trend is connected with decreasing average radius of the creaming species, as predicted by the theory (compare with Fig. 2b). Smaller objects experience lower gravitational force, so the process of creaming becomes slower. The measured mean radii of the single drops in the three emulsions (Figs. 4a–4d) are almost the same, 3.0–3.2 μm, so the differences in the creaming rates can be attributed solely to the different degree of flocculation. The latter has a great impact to practice, since it determines the texture of the commercial products.

Obviously, rising protein concentration enhances the stability against creaming and flocculation. Since in all cases the quantity of the protein is at least enough to cover the oil/water interfaces (see below), and there is no coalescence, we can conclude that the presence of *excess* protein hampers the flocculation, which is manifested as a decrease in the average number of droplets in a floc. We have carried out preliminary investigations of thin liquid films made in a glass capillary and observed by means of interference microscopy. The results show that BLG often forms aggregates with submicrometer size, which reside on the liquid boundary. A sample picture of a thin film is presented in Fig. 5c—the protein lumps are clearly seen. Moreover, Dickinson (4) mentioned that adsorbed BLG undergoes unfolding and slow polymerization, and the surface coverage and the layer thickness gradually increase with time. The ability of globular proteins to aggregate as a result of their partial denaturation on the interface was discussed in Ref. 14. Most probably, in our o/w emulsions augmented steric repulsion of the lumps and/or multilayers adsorbed on the drop surfaces obstructs the formation of tightly packed aggregates at increased protein concentrations.

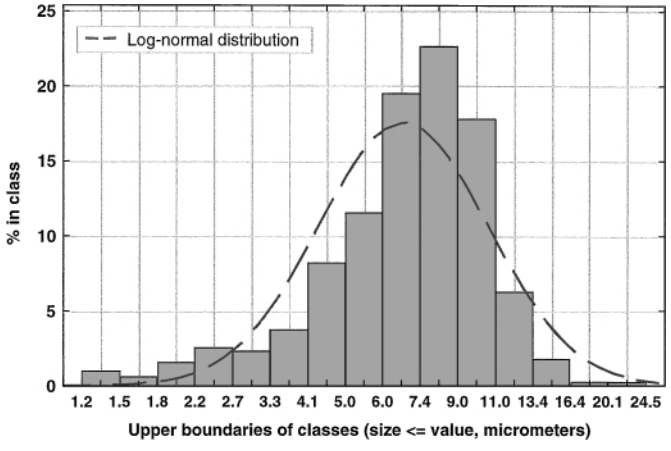

FIG. 6. A sample histogram for the size distribution of emulsion droplets in a system containing 0.2 wt% BLG + 0.15 M NaCl at pH 7 (row 3 in Table 1). 512 drops were counted; the diameter was measured by means of light microscopy.

TABLE 1
Type of Creaming for Different Batch Emulsions and the Fitting Parameters (a_{eff}, $\tilde{p}_0$, ϕ_{max}) in the Case of SB (Sharp Boundary) Mechanism

No.	System	a_{eff} (μm)	ϕ_{max}	ϕ_{exper}	$\tilde{p}_0$	Note
1	0.05 wt% BLG $I = 0.156$ M, pH 7.0 Xylene	11.40	0.58	0.56	1.3×10^{-3}	$R_1 = 3$–3.2 μm Flocculated $N = 32 \pm 7$
2	0.10 wt% BLG $I = 0.156$ M, pH 7.0 Xylene	10.72	0.58	0.56	1.3×10^{-3}	$R_1 = 3$–3.2 μm Flocculated $N = 26 \pm 7$
3	0.20 wt% BLG $I = 0.156$ M, pH 7.0 Xylene	7.91	0.57	0.56	1.3×10^{-3}	$R_1 = 3$–3.2 μm Flocculated $N = 11 \pm 5$
4	0.02 wt% BSA-FAF $I = 0.156$ M, pH 7.0 Xylene	24.50	0.74	0.70	1.3×10^{-3}	$R_1 = 3$–3.5 μm Flocculated $N = 315 \pm 50$
5	0.02 wt% BSA-FAF $I = 0.156$ M, pH 7.0 Soybean oil	20.60	0.74	0.70	6.5×10^{-4}	$R_1 = 3$–3.5 μm Flocculated $N = 188 \pm 50$
6	0.02 wt% BLG + β-casein (1 : 3); $I = 0.156$ M, pH 5.3 Xylene	Cannot be fitted				Single drops mainly
7	0.02 wt% BLG + β-casein (1 : 1); $I = 0.156$ M, pH 5.3 Xylene	12.26	0.80	0.75	3.0×10^{-4}	Single drops mainly
8	0.02 wt% BLG + β-casein (3 : 1); $I = 0.156$ M, pH 5.3 Xylene	7.26	0.80	0.75	1.3×10^{-3}	Single drops mainly
9	0.02 wt% BSA-non-FAF $I = 0.156$ M, pH 7.0 Soybean oil					
10	0.05 wt% BSA-non-FAF $I = 0.156$ M, pH 7.0 Soybean oil	Diffuse boundary (DB mechanism)				
11	0.05 wt% β-casein $I = 0.156$ M, pH 5.3 Soybean oil	Turbid serum phase (presence of small nonflocculating droplets)				
12	0.20 wt% β-casein $I = 0.156$ M, pH 5.3 Soybean oil					

Note. N is the average number of droplets in a floc, and R_1 is the radius of the individual drop. The two different numbers for R_1 given in the last column of the table correspond to the lower and upper limits of the confidence interval for the mean diameter, with the level of certainty 95% (obtained by statistical averaging from size distribution data (see, e.g., Fig. 6)).

The absolute error of the data presented in Fig. 4 is contained approximately within the size of the points. The corresponding error in the effective radius of the sedimenting species (in the theoretical fit) is about ± 0.3 μm. It is true that the creaming results for 0.05 and 0.1 wt% BLG (Figs. 4a and 4b) are quite close. Evidently, the anti-flocculating action of the excess amount of protein becomes considerable only at relatively higher concentrations (e.g., 0.2 wt%, Figs. 4c and 4d).

Figure 5a demonstrates that the drops engaged in a floc are very slightly deformed.This is an indication for absence of strong interdroplet attraction (although there is still sufficient attraction to keep the drops together and prevent floc disintegration). It is likely that the emulsions are flocculated by protein bridges.

Let us now pay attention to the role of pH for the properties of emulsions stabilized by BLG. In addition to the studies at pH 7 (Table 1), experiments at pH 5.4 (the isoelectric point of BLG, IP) have also been performed. It was found that the rate of creaming, the final volume of the cream, and the mean droplet size were equal in the two series of measurements. However, a difference connected with coalescence emerges during the *secondary creaming* (cf. Section 4 for explanation of the experimental procedure). When pH is equal to 7.0, a "coarse cream" layer appears on top of the samples after the mechanical agitation, whereas at the lower pH such a layer does not form. The "coarse cream" is composed of much larger emulsion droplets (millimeter size), produced as a result of coalescence. The latter

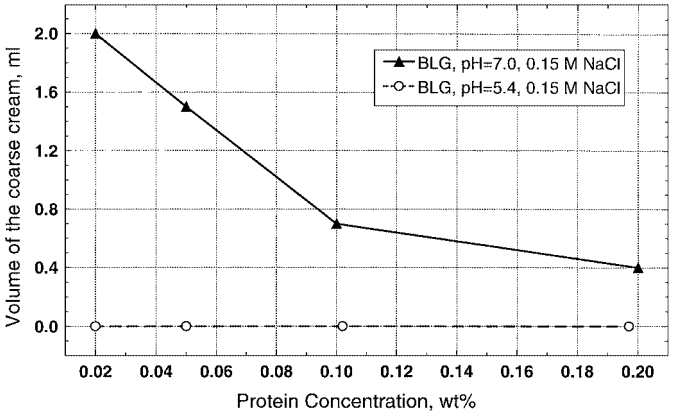

FIG. 7. Quantity of the coarse cream, released in batch emulsions stabilized with BLG, at pH 5.4 and 7.0.

is induced by the impact of the gentle shear when the already creamed emulsion is shaken. Since the only difference between the samples with and without coarse cream was the pH, we can infer that the particular conformation of the protein (which is strongly pH-dependent) is of great importance for the stability against rupture of the intervening thin liquid layer between the drops. Probably, at pH close to the IP the interfacial adsorption layers are more stiff. These effects are illustrated in Fig. 7, from which one sees that at pH 7 increasing protein concentration hampers the coalescence.

We have never observed coalescence during the *primary* creaming. The droplet size distribution was measured immediately after homogenization of the emulsion and 4 h later (in systems with BLG, at pH 7.0, with 0.15 M NaCl, at different protein concentrations). No significant change in the mean radius of the drops, R_1 , was detected. Therefore, mechanical agitation turns out to be a prerequisite for drop rupture. The experiments show that the rate of *secondary* creaming is not very different for pH 5.4 and pH 7.0 (despite the coalescence in the latter case). Perhaps, the size of the drop clusters produced during the emulsion shaking after the primary creaming is the main factor that determines the secondary creaming behavior. In addition, there is little difference (with respect to the rate of sedimentation) between a floc with a certain radius and a large drop of the same size, formed as a result of coalescence.

5.1.2. BSA-fatty acid free (FAF). The mechanism of creaming of emulsions stabilized by BSA-FAF is found to be the same as that in the case of BLG (see Fig. 4e). However, an important difference in the size of the flocs exists (compare rows 4, 5, and 1–3 in Table 1). The average number of droplets in a floc in BSA-FAF containing emulsions is several times bigger than the average droplet number in the case of BLG. This inference is qualitatively supported by microscopic observations: the samples with BSA-FAF are very strongly flocculated, and huge clusters of many droplets are seen (but in such 3D flocs the individual droplets cannot be clearly discerned).

In addition, the oil volume fraction in the cream is higher with BSA-FAF than with BLG (Table 1 and Fig. 8b). Therefore, the cream and the flocs with BSA-FAF are more tightly packed, which is evident also from the fact that the final volume of the cream is smaller with BSA-FAF compared to BLG (Fig. 8a).

The change of the oil phase (xylene–soybean oil) does not alter significantly the creaming behavior of the emulsions containing BSA-FAF, as is clear from Fig. 4e.

5.1.3. BLG + β-casein mixtures. In order to achieve a better understanding of the effect of protein type, we performed some experiments with emulsions stabilized by mixtures of BLG and β-casein, keeping the total concentration equal to 0.020 wt% in all cases. Pure β-casein systems exhibit a specific creaming behavior, different from the SB type, which will be further called DB (diffuse boundary) mechanism (see below for description). β-Casein is a disordered protein, frequently considered as intermediate between the stochastic random-coil polymers and well organized structures such as globular proteins (a group that BSA and BLG belong to). We have found that in the studied mixtures of BLG and β-casein the emulsion creaming follows the SB mechanism (rows 6–8 in Table 1). However, when β-casein is in excess (3 : 1, row 6), the experimental creaming curve cannot be fitted with our theory. Probably, some of the basic assumptions in the model cease to be valid. The fit for the case of BLG : β-casein = 3 : 1 (Fig. 4f) is better than that for 1 : 1

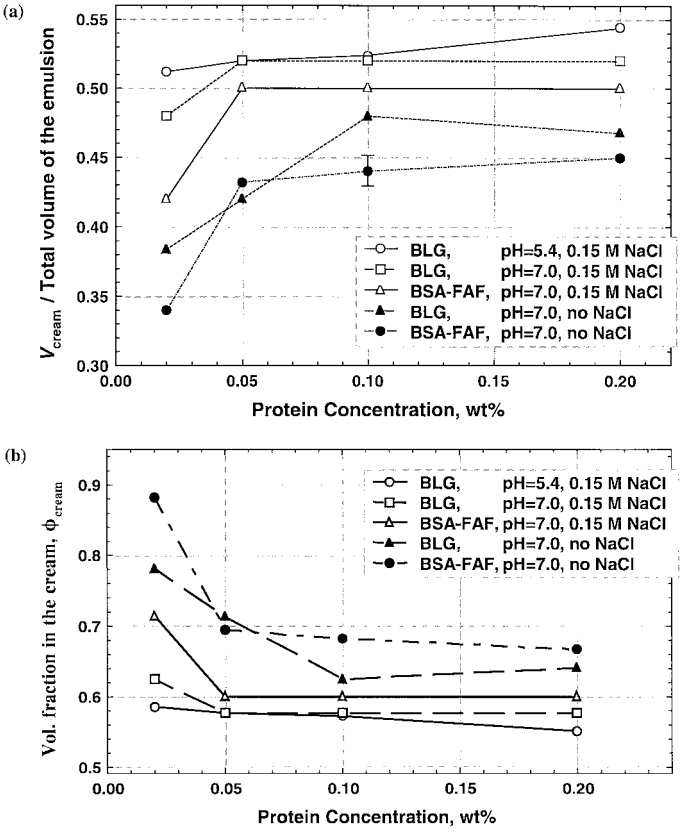

FIG. 8. (a) Volume of the separated cream phase in the final state (after ∼1000 min), scaled with the total emulsion volume, and (b) the corresponding oil volume fraction in the cream, in the cases when the process of creaming is governed by the SB mechanism.

(not shown). There seems to be a gradual transition in the behavior of the emulsions—they depart from the SB type of creaming with increasing β-casein content.

An important observation here is that the mean radius of the individual droplets in the mixed systems is about 8–15 μm, i.e., considerably larger than the mean drop radii with BLG, BSA-FAF, and β-casein alone (see below for the latter case). One possible reason for this peculiarity of the mixtures may be connected with competition between the proteins during emulsification, accompanied by bridging. Perhaps the temporary contacts between the drops in the first moments are less stable in the mixed systems, hence quick coalescence occurs. The comparison of the average size of the creaming species, found from the fit (Fig. 4f; rows 7, 8 in Table 1), and the radius of the individual droplets (measured experimentally) reveals that there is practically no flocculation in the final dispersion: the creaming objects are single drops.

The differences in the drop size could also be due to different adsorption kinetics (at relatively short times). The qualitative disparity in the extent of flocculation can be attributed to the interactions between the protein molecules and the sticking ability of the surfaces. An important aspect of the protein properties related to flocculation is the formation of aggregates. BLG in bulk aqueous solutions has been shown to exist mainly in the form of small clusters (dimers to octamers, whose size is of the order of several nanometers) (14). In contrast, β-casein and its mixtures with BLG give large ($\sim$300 nm) and polydisperse aggregates (15) and our own measurements with dynamic light scattering). Such big lumps (and even larger) are also present on the interfaces (a fact confirmed by direct observations of thin liquid films in a capillary cell (16)). They could play a major role in preventing flocculation.

5.1.4. Final State of the Cream. Let us now comment briefly on Fig. 8, which presents the final volume of the separated cream at long times (Fig. 8a), and the corresponding average oil volume fraction (Fig. 8b) in all cases of emulsions obeying the SB mechanism and stabilized by individual proteins. For all samples it is true that the cream is most tightly packed at the lowest concentration of protein, 0.02 wt% (Fig. 8b). The diminishing ϕ_{cream} with rising concentration may be attributed to increasing stiffness of the surfaces and reduced ability for rearrangement of the particulate network. At 0.02 wt% the total quantity of the protein is sufficient to cover the interfaces with a firm monolayer (see below). Increasing protein content leads to denser layers and adsorption of multilayers and protein lumps, responsible for looser packing of the cream at 0.05, 0.10, and 0.20 wt%.

The droplet size distribution in some emulsion samples was measured by us using light microscopy. One histogram is shown in Fig. 6; it is a result from counting of 512 droplets. (Let us mention that the data presentation in Fig. 6, with columns referring to size classes in a logarithmic scale on the abscissa, already implies some averaging of the original measured sizes within the classes.) The mean value of the drop diameter is estimated from a statistical analysis: we have used the software package *Statistica* (StatSoft, Inc., OK, USA) to process the original experimental data. In such a manner the numbers for R_1 in Table 1 were obtained. Besides, the size distributions in our systems are satisfactorily represented by log-normal curves (which are known to be appropriate for emulsions) (see Fig. 6).

The data for R_1 give information about the specific surface area (the total area of the oil/water interfaces of the drops per unit volume of the oil phase). The result is 6.33×10^3 cm^{-1} for systems containing BLG at different concentrations (since the drop radius R_1 does not vary with the protein content (cf. Table 1), we may accept that the above value of the specific surface area is pertinent for all studied emulsions with BLG). Taking into account that the oil volume fraction is 0.3, we can now estimate the maximum attainable adsorption, Γ, for a given protein concentration in the aqueous phase. Thus, at 0.02 wt% the protein amount is sufficient to ensure $\Gamma = 0.74$ mg/m^2; at 0.05 wt% $\Gamma = 1.84$ mg/m^2, and so on. According to Atkinson *et al.* (17), the dense layer of adsorbed BLG has $\Gamma \approx 1.6$ mg/m^2. Although it seems that at 0.02 wt% the protein is not enough to cover the interfaces tightly, our emulsions are *stable* against coalescence (see the remark at the end of Section 5.1.1). Indeed, as pointed out by Dalgleish (18), emulsions are often stable with less than the maximal amount of protein which covers the o/w boundaries at saturation.

Another important observation from Fig. 8 (already mentioned in Section 5.1.2) is that the cream with BSA-FAF is more closely packed compared to the case with BLG. At higher ionic strength the volume of the cream is larger (Fig. 8a), and ϕ_{cream} is smaller (Fig. 8b). This of course should be expected, in view of the suppression of the electrostatic repulsion: With more salt the films (or gaps) between the droplets in the flocs are thinner, the surfaces are less mobile, and rearrangement and compactification inside the cream is blocked.

5.2. Creaming with Diffuse Boundary (DB Mechanism)

This mechanism is characterised by absence of a clear serum phase. Instead, the whole emulsion column is turbid, and the volume fraction changes gradually in vertical direction. No detectable boundaries between distinct layers can be observed with the naked eye (at least for not very long times after the creaming starts), in contrast to the previous case of SB mechanism. Very small (nonflocculated) droplets float in the lower part of the emulsion sample, whereas the larger drops are collected in the upper cream. To quantify this behavior is much harder in comparison with the SB type. The studied systems which cream according to the DB mechanism are listed in Table 1.

In a system stabilized by BSA-non-FAF we took a sample from the bottom of the column and carried out a dynamic light scattering measurement (with the help of the Malvern 4700C apparatus), which gave us the mean size of the present species in the serum phase. The samples were not diluted, in order to preclude contingent coalescence caused by hydrodynamic fluxes. In the obtained differential distribution curve a population of small

objects with mean diameter of ca. 400 nm could be discerned. We performed a light scattering study of aqueous solutions of BSA-non-FAF, and proved that this protein does not form aggregates in the bulk. Therefore, we can safely accept that the detected objects in the serum phase represent submicrometer emulsion droplets.

It is worthwhile noting the difference between the creaming mechanisms of emulsions stabilized with BSA-FAF and BSA-non-FAF (with all other conditions being the same). As has already been mentioned, for BSA-FAF the process of creaming is governed by the SB mechanism, while the presence of BSA-non-FAF brings about creaming according to the DB mechanism. Since the individual droplets in the two cases are found to be of almost the same average size ($\sim 3\ \mu$m, Table 1), it is evident that the great difference in the macroscopic behavior originates from the flocculation of the samples. The latter is more pronounced with BSA-FAF. We can infer that absence of fatty acids built in the BSA molecule somehow enhances the flocculation.

Batch emulsions stabilized with pure β-casein definitely follow the DB mechanism (see rows 11, 12 in Table 1), in the whole range of studied concentrations. This is an important result, because emulsions containing mixtures of β-casein and BLG show creaming behavior qualitatively similar to that of pure BLG (sharp boundary, SB mechanism). Neither with pure β-casein nor with the mixtures is the flocculation very intensive (rows 6–8, 11, 12 in Table 1). However, much smaller drops exist in the emulsion with β-casein only. This leads to increased stability against creaming. Figure 5b presents a microscopic image of an emulsion sample containing 0.05 wt% β-casein. The droplets are essentially nonflocculated; sometimes it is seen that neighboring drops (which may look connected) separate from each other. This can be compared to the case of BLG (Fig. 5a), when the drops stay attached firmly and irreversibly, and are even slightly deformed to the extent that small films exist between them. The direct observation thus supports the conjecture that the DB mechanism of creaming (typical for β-casein alone) is associated with the presence of small nonflocculating droplets.

6. ORTHOKINETIC FLOCCULATION OF MICROMETER-SIZE EMULSION DROPS

In this section we provide evidence that the buoyancy-driven flocculation of micrometer-size emulsion droplets is a fast process, and therefore, it will already be completed before a macroscopically appreciable creaming takes place.

6.1. Formulation of the Problem

Let us consider a dispersion in which spherical particles of different radii move upward due to gravity. Larger particles move faster, reach the smaller ones and collide with them. In this manner aggregates are formed. We shall be interested in a theoretical modeling of the changes in the size distribution with time. Basically, the considerations of Reddy *et al.* (19) will be followed. We accept some simplifying assumptions:

(i) The drops move along one axis (z) only; rotation is neglected.

(ii) Each collision leads to irreversible formation of a larger particle; i.e., the collision efficiency is 100%, there is no fragmentation. We also discard the possibility for coalescence, in other words, only flocs of the initially available drops exist at later times. This is important for the discretization of the problem (see below).

(iii) The particles are big enough so that the Brownian motion is immaterial.

(iv) All flocs are assumed to be spherical; they are packed at a fixed volume fraction, ϕ^*, which is equal to the average final value of ϕ in the cream.

(v) It is impossible to obtain flocs larger than a given size (upper cutoff). Our experimental observations in real systems have shown that typically there are no aggregates bigger than 8–10 μm in radius. Most probably, larger clusters are hydrodynamically unstable and disintegrate at the moment of formation.

In steady state the buoyancy balances the viscous drag exerted on each particle (floc). For the ith object (whose radius is R_i) we write

$$6\pi\eta R_i v_i = \frac{4}{3}\pi R_i^3 \Delta\rho g K(\phi), \qquad [15]$$

where v_i is the particle velocity, and the other notation is the same as in Section 2. Thus,

$$v_i = \frac{2\Delta\rho g}{9\eta} K(\phi) R_i^2 = A R_i^2. \qquad [16]$$

Here we introduce the constant A, which contains physical parameters of the system and does not depend on the size distribution. The relative velocity of the jth object with respect to the ith one is

$$v_{ij} = v_j - v_i = A\left(R_j^2 - R_i^2\right). \qquad [17]$$

The difference in the velocities leads to collision and, consequently, to flocculation. Let us calculate the flux, $Q_y(i, j)$, of particles j which hit upon the central particle i (Fig. 9). If the center of the jth object (coming from above, to strike the plane of the drawing in Fig. 9) falls into the circle of radius $R_{ij} = R_i + R_j$, then collision will occur. The flux in the segment of area $2\sqrt{R_{ij}^2 - y^2}\,\mathrm{d}y$ along the y axis (shaded in Fig. 9) is:

$$\mathrm{d}Q_y(i, j) = 2|v_{ij}|\sqrt{R_{ij}^2 - y^2}\,\mathrm{d}y. \qquad [18]$$

After integration of Eq. [18] with respect to y, from $(-R_{ij})$ to R_{ij} (Fig. 9), and substitution with Eq. [17] for v_{ij}, we find the total flux in the form

$$Q_y(i, j) = A\pi(R_i + R_j)^2\left|R_j^2 - R_i^2\right|. \qquad [19]$$

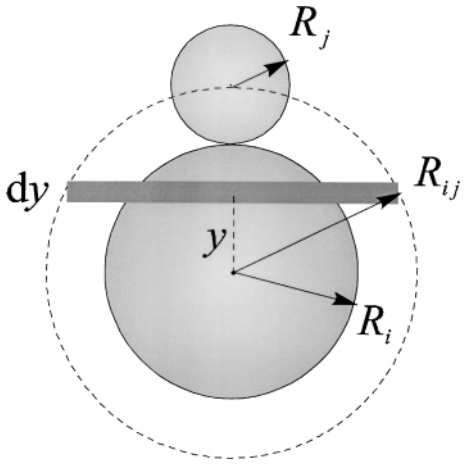

FIG. 9. Sketch of the area of contact for two emulsion droplets with different radii, R_i, R_j.

Let us now consider the aggregation process. Hereafter C_k will denote the number concentration of aggregates comprising k individual drops. The number of collisions of particles j with one particle of type i per unit time is $C_j Q_y(i, j)$. The kinetics of aggregation is described by the following differential equation (19),

$$\frac{dC_k}{dt} = \frac{1}{2}\sum_{i=1}^{k-1} C_i C_{k-i} Q_y(i, k-i) - \sum_{i=1}^{\infty} C_i C_k Q_y(i, k), \quad [20]$$

where the first term in the right-hand side accounts for the formation of aggregates. The second term represents the decrease of C_k due to further aggregation of the particles k, forming larger clusters. Inserting $Q_y(i, j)$ into Eq. [20], one obtains a set of nonlinear differential equations:

$$\frac{dC_k}{dt} = \frac{1}{2}\sum_{i=1}^{k-1} C_i C_{k-i} A\pi (R_i + R_{k-i})^2 \left|R_i^2 - R_{k-i}^2\right| - \sum_{i=1}^{\infty} C_i C_k A\pi (R_i + R_k)^2 \left|R_i^2 - R_k^2\right|. \quad [21]$$

The size distribution at $t = 0$ defines the initial conditions for all C_k.

6.2. Solution and Discussion

Each equation of the set [21] is nonlinear, and one has to be careful with the numerical treatment of the problem. The droplets (aggregates) are of micrometer size, so the magnitude of each R_i is about 10^{-4} cm. The number concentrations could be of the order of 10^7 cm^{-3}. This huge difference in the values could evoke numerical instability when the quantities are multiplied. For that reason one needs to reformulate the problem in order to apply an integration scheme.

In the case of an emulsion whose individual drops are polydisperse, it is feasible to classify the particles (flocs) in groups, each of them comprising a given number of droplets and having a *mean* radius R_i. Since all flocs are supposedly packed with one and the same volume fraction, ϕ^*, the effective radius, R_F, of a floc which contains N drops will be

$$R_F(N) = R_1 \sqrt[3]{N/\phi^*}. \quad [22]$$

Let α_i be the volume fraction of the group i, with respect to the total oil content in the emulsion. Then

$$\alpha_i = \frac{4\pi}{3\phi} C_i R_i^3. \quad [23]$$

Switching over from C_k to α_k in Eqs. [21], with the help of Eq. [23], we arrive at

$$\frac{d\alpha_k}{dt} = \frac{\pi A}{2s}\sum_{i=1}^{k-1} \alpha_i \alpha_{k-i} \frac{(R_i + R_{k-i})^2 \left|R_i^2 - R_{k-i}^2\right| R_k^3}{R_{k-i}^3 R_i^3} - \frac{\pi A}{s}\sum_{i=1}^{N_m} \alpha_i \alpha_k \frac{(R_i + R_k)^2 \left|R_i^2 - R_k^2\right|}{R_i^3}, \quad [24]$$

where N_m is the maximum possible number of drops in a floc, and $s = 4\pi/(3\phi)$ is a parameter. It is easy to see that $\sum_{i=1}^{N_m} \alpha_i = 1$, and $0 \le \alpha_i \le 1$. The set of differential Eqs. [24] is more convenient for numerical computation than Eqs. [21].

The system [24] was integrated applying a fourth-order Runge–Kutta scheme (12). In the initial moment $t = 0$ we suppose that particles with $N = 1$, 2, and 3 are present, so that the average diameter of the objects in the dispersion is about 3 μm.

Figure 10 illustrates the time evolution of the volume fractions of several groups of droplets. The calculation has been

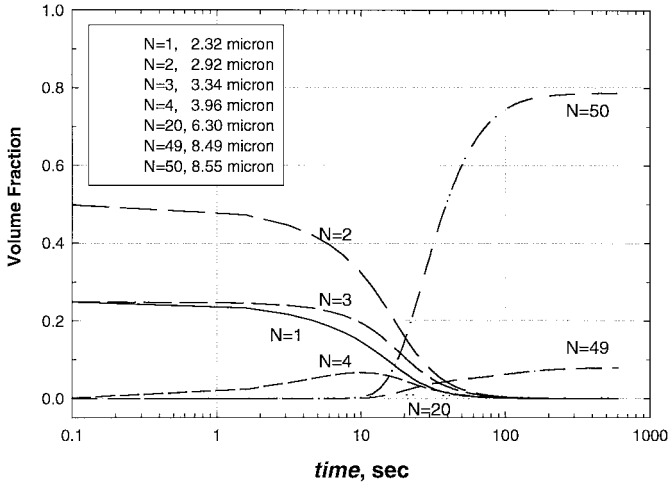

FIG. 10. Volume fractions of different aggregates (containing N droplets) in a flocculating emulsion, plotted vs time (numerical simulation).

performed with a size distribution which includes 50 fractions. The maximum floc radius is 8.55 μm, and the minimum one is 2.3 μm (single drop). One can see that after the 100th second the composition of the suspension practically does not change (the concentrations of all species reach plateaus). The majority of the droplets are included in the biggest flocs, $N = N_m = 50$. The fact that the final flocculated state is reached relatively fast is in good agreement with our creaming results, which comply with the model from Section 2. We have supposed that the process of aggregation is practically finished before macroscopically appreciable creaming occurs. This assumption is now confirmed (in the absence of potential barriers for flocculation).

7. CONCLUSIONS

In this work we consider the rate of creaming of batch emulsions when a sharp boundary between the dispersion and a clear serum layer exists (SB mechanism). Physically, the process of creaming is represented as a continuous consolidation of a partially aggregated network. Our treatment is based on works of other authors (8, 9), who derived a partial differential equation for the time evolution of the local volume fraction. We formulate a complete mathematical problem by imposing appropriate boundary and initial conditions and perform numerical calculations. As a result, the position of the boundary between the serum and the concentrated emulsion is obtained as a function of time. The observed trend for gradually decreasing rate of sedimentation as time goes on is reproduced correctly by the theory. The predictions of the latter are compared with direct experimental measurements of the creaming rate in o/w emulsions stabilized by proteins. Systems containing BSA, BLG, and β-casein have been investigated. The experimental data for the time dependence of the position of the serum/emulsion boundary are fitted by adjusting the model parameters in the theory, and very good agreement is obtained. The results allow us to interpret the differences in the rate of creaming in terms of different extent of flocculation of the emulsion drops. The effective size of the particles (flocs) from which the emulsion is composed is found both from the calculations and by microscopic observation. The presence of larger particles brings about faster sedimentation: the creaming curve retains its shape (in log(time) scale), but shifts to the shorter times.

The creaming of emulsions with BLG, BSA-FAF, and mixtures BLG + β-casein follows the SB mechanism (and can be explained as consolidation of a particulate network). These dispersions contain flocs, which are smaller when the protein concentration is higher. The latter fact supports the hypothesis for the stabilizing role of the excess amount of protein (forming lumps and multilayers on the interface, which perhaps gives rise to steric repulsion effects).

Theoretical analysis demonstrates that the formation of flocs by the mechanism of gravitational coagulation is a much faster process than the consolidation of the cream. Hence, systems in which there is no potential barrier for aggregation will first flocculate, and then cream. This happens in our systems obeying the SB mechanism.

The emulsions stabilized by mixtures of BLG and β-casein exhibit definitely larger mean drop radius in comparison with the systems containing the individual proteins. Moreover, the mixed samples do not flocculate. With changing composition there seems to be a gradual transition in the behavior of the emulsions—they depart from the SB mechanism when the content of β-casein increases. Perhaps, this is connected with an augmented ability of β-casein to prevent droplet aggregation. Creaming of emulsions containing pure β-casein (and pure BSA non-FAF) is characterized by the presence of small nonflocculated droplets, which would not sediment ("diffuse boundary" mechanism, DB). Such systems are therefore more stable against creaming.

ACKNOWLEDGMENTS

This work was financially supported by Kraft Foods, Inc., and partially by the Laboratoire Franco-Bulgare. Fruitful discussions with Professor Ivan B. Ivanov are highly appreciated.

REFERENCES

1. Dickinson, E., Golding, M., and Povey, M. J. W., *J. Colloid Interface Sci.* **185,** 515–529 (1997).
2. Dickinson, E., Ritzoulis, C., and Povey, M. J. W., *J. Colloid Interface Sci.* **212,** 466–473 (1999).
3. Manoj, P., Fillery-Travis, A. J., Watson, A. D., Hibberd, D. J., and Robins, M. M., *J. Colloid Interface Sci.* **207,** 283–293 (1998).
4. Dickinson, E., *J. Chem. Soc. Faraday Trans.* **94**(12), 1657–1669 (1998).
5. Pinfield, V. J., Dickinson, E., and Povey, M. J. W., *J. Colloid Interface Sci.* **186,** 80–89 (1997).
6. Friberg, S. E., and Yang, J., *in* "Emulsions and Emulsion Stability" (J. Sjoblom, Ed.), Chap. 1, p. 1. Dekker, New York, 1996.
7. Dukhin, S., and Sjoblom, J., *in* "Emulsions and Emulsion Stability" (J. Sjoblom, Ed.), Chap. 2, p. 41. Dekker, New York, 1996.
8. Buscall, R., *Colloids Surf.* **43,** 33–53 (1990).
9. Buscall, R., and White, L. R., *J. Chem. Soc. Faraday Trans. I* **83,** 873–891 (1987).
10. Landman, K. A., and White, L. R., *Adv. Colloid Interface Sci.* **51**(1–3), 175–246 (1994).
11. Russel, W. B., Saville, D. A., and Schowalter, W. R., "Colloidal Dispersions," Chap.12. Cambridge Univ. Press, Cambridge, 1989.
12. Constantinides, A., "Applied Numerical Methods with Personal Computers." McGraw–Hill, New York, 1987.
13. Gaonkar, A. G., *J. Am. Oil Chem. Soc.* **66,** 1090 (1989).
14. Lefebvre, J., and Relkin, P., *in* "Surface Activity of Proteins" (S. Magdassi, Ed.), Chap. 7, p. 181. Dekker, New York, 1996.
15. Pankratova, M. N., Bobrova, L. E., Bolobova, A. V., and Izmailova, V. N., *Kolloidn. Zh.* **36,** 54–57 (1974).
16. Velev, O. D., Campbell, B. E., and Borwankar, R. P., *Langmuir* **14**(15), 4122–4130 (1998).
17. Atkinson, P. J., Dickinson, E., Horne, D. S., and Richardson, R. M., *J. Chem. Soc. Faraday Trans.* **91**(17), 2847–2854 (1995).
18. Dalgleish, D. G., *in* "Food Emulsions and Foams" (E. Dickinson and J. M. Rodriguez Patino, Eds.), p. 1. Royal Soc. Chem., Cambridge, 1999.
19. Reddy, S. R., Melik, D. H., and Fogler, H. S., *J. Colloid Interface Sci.* **82,** 116 (1981).